This article was downloaded by:
On: *18 January 2011*
Access details: *Access Details: Free Access*
Publisher *Taylor & Francis*
Informa Ltd Registered in England and Wales Registered Number: 1072954 Registered office: Mortimer House, 37-41 Mortimer Street, London W1T 3JH, UK

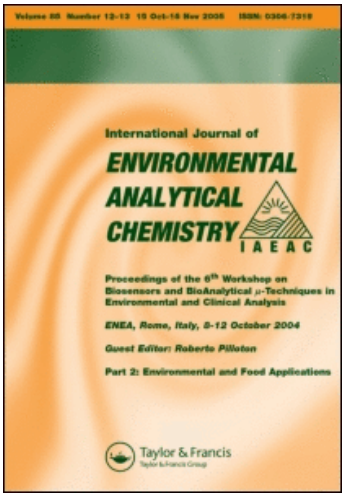

International Journal of Environmental Analytical Chemistry
Publication details, including instructions for authors and subscription information:
http://www.informaworld.com/smpp/title~content=t713640455

Characterization of Oil Fly Ash Particles by Electron Probe Microanalysis

B. Raeymaekers[a]; M. Demuynck[ab]; W. Dorrine[a]; F. Adams[a]
[a] Department of Chemistry, University of Antwerp (UIA) Universiteitsplein 1, Wilrijk, Belgium [b] Studiecentrum voor Ekologie en Bosbouw (LISEC), Genk, Bokrijk

To cite this Article Raeymaekers, B. , Demuynck, M. , Dorrine, W. and Adams, F.(1988) 'Characterization of Oil Fly Ash Particles by Electron Probe Microanalysis', International Journal of Environmental Analytical Chemistry, 32: 3, 291 — 312
To link to this Article: DOI: 10.1080/03067318808079119
URL: http://dx.doi.org/10.1080/03067318808079119

PLEASE SCROLL DOWN FOR ARTICLE

Full terms and conditions of use: http://www.informaworld.com/terms-and-conditions-of-access.pdf

This article may be used for research, teaching and private study purposes. Any substantial or systematic reproduction, re-distribution, re-selling, loan or sub-licensing, systematic supply or distribution in any form to anyone is expressly forbidden.

The publisher does not give any warranty express or implied or make any representation that the contents will be complete or accurate or up to date. The accuracy of any instructions, formulae and drug doses should be independently verified with primary sources. The publisher shall not be liable for any loss, actions, claims, proceedings, demand or costs or damages whatsoever or howsoever caused arising directly or indirectly in connection with or arising out of the use of this material.

Intern. J. Environ. Anal. Chem., Vol. 32, pp. 291–312
Reprints available directly from the publisher
Photocopying permitted by licence only
© 1988 Gordon and Breach, Science Publishers, Inc.
Printed in Great Britain

Downloaded At: 19:16 18 January 2011

Characterization of Oil Fly Ash Particles by Electron Probe Microanalysis

B. RAEYMAEKERS, M. DEMUYNCK*, W. DORRINE and F. ADAMS

Department of Chemistry, University of Antwerp (UIA) Universiteitsplein 1, B-2610 Wilrijk, Belgium

(*Received 13 August 1987; in final form 5 September 1987*)

An automated electron microprobe was used to characterize more than 25 000 fly ash particles with diameters between 1 μm and 200 μm, which were collected in two fractions from the stack of an oil fired power plant under two different burning conditions. Sample preparation procedures were developed to insure a quantitative particle transfer from the collection container to a Nuclepore filter and the automated localization of the carbonaceous particles in the backscattered electron image was optimized. Size distributions were measured and the results were interpreted in terms of the burning conditions of the power plant.

KEY WORDS: Electron probe micro analysis, particle characterization, fly ash, carbonaceous particles.

INTRODUCTION

There is at present much interest in the characteristics of oil fly ash particles, generated in oil fired power plants, especially because they commonly contain high concentrations of soot, sulphates and metals. The interdependence of acid rain, the deterioration of historical

*Studiecentrum voor Ekologie en Bosbouw (LISEC) 3600 Genk-Bokrijk.

monuments and the presence of fly ash in the environment was reviewed recently.[1] Also, the general characteristics of oil fly ash particles can be a valuable indicator for monitoring the burning process within the power plant. The optimization of burning processes has been intensively studied and the reduction of soot and sulphur oxide emissions were the primary goal of experiments on different power plants as was e.g. described by Cramer *et al.*, 1977.[2]

Chemical and morphological characteristics of individual fly ash particles were intensively studied during the last decade, using mostly analytical electron microscopy,[3] but also laser microprobe mass analysis,[4] has been employed to determine the composition of individual particles. These methods normally yield only data on a limited number of particles as selected by the operator of the instrument and therefore, the reported characteristics are not always representative for the entire particle population. Moreover, the manually controlled characterization of larger particle collections of in excess of a hundred particles is a very elaborate job with a high laboratory-economical cost.

Downloaded At: 19:16 18 January 2011

Computer controlled electron microprobes were developed for automated particle characterization and these can perform on-line image analysis.[5] These methods can analyse thousands of particles within a reasonable time e.g. a full working day. A disadvantage of automated particle analysis is the loss of the operator's experience, so that information of the fine particle texture or the recognition of any particles with anomalous shape or composition does not become available. On the other hand, the advantages of such an approach are manifold, amongst others:

—the particles subjected to analysis are selected randomly, improving the representativity of the analysis and excluding any bias of selection generated by the operator.

—standard imaging procedures guarantee a reproducible particle localization.[6]

—large numbers of particles can be analysed without any human intervention, e.g. during low activity periods on the laboratory schedule, e.g. at night or during weekends.

In this study, an automated electron microprobe as described previously,[7] was used to characterize oil fly ash particles from a

power plant that were sampled in two individual size fractions namely by a cyclone and a backup filter. It was the aim of this study to develop a method for a representative characterization of carbonaceous particles and to gather statistically reliable information on the influence of the burning conditions on the characteristics of the fly ash emitted.

EXPERIMENTAL

The automated EPMA analysis of microparticles developed in our laboratory,[7,8] yields data on the size and composition of a large number of particles without any operator's intervention. The electron beam is scanned across a pixel raster over the sample and localizes objects with closed contours that show an image intensity higher than a preselected threshold value. When a single particle is completely localized, an X-ray spectrum is acquired. The particle size and the X-ray peak intensities are then calculated. After the analysis, all analytical data are processed to obtain size distributions and the composition of each individual particle.

An image with an excellent contrast between the particles and the substrate on which they are dispersed is needed to allow a reliable characterization. This is especially problematic for the analysis of carbonaceous particles which cannot easily be localised accurately on the substrate. Indeed, as the mean atomic number of the fly ash particles and that of commonly used substrates are similar, a poor contrast is obtained in the backscattered electron image. A better contrast could be obtained in the secondary electron image, but then the image intensity fluctuates strongly within the particle contour, resulting often in the detection of a single particle as several distinct entities. It appeared that excellent high contrast images were produced by dispersion of the particles on a silver coated Nuclepore filter. The backscattered electron image then showed black contours of low atomic number compared with the substrate which coincided with the shape of the particles. In the inverted backscattered electron image, uniform and reproducible particle images were obtained at an electron beam energy of 15 keV, as shown in Figure 1. Characteristic features are the fluffy shadows around the actual contours. These shadows originate from the detection geometry, in which the sub-

Downloaded At: 19:16 18 January 2011

strate area around the particles is shielded by the particle from the annular backscattered electron detector. A typical image profile with a threshold position for correct size determination is shown in Figure 2. Finally, Figure 3 illustrates the accuracy with which these particles can be localized.

X-ray spectra are acquired while the electron beam performs a raster scanning over the particle surface, so that the electron dose is spread uniformly over the object. Net peak intensities are calculated by a fast derivative algorithm,[9] and a standardless ZAF correction procedure is used to calculate particle composition from the net X-ray peak intensities.[10]

The particles belonging to the filter fraction did not generate problems because they are practically all compact items with a homogeneous texture, for which elemental concentrations can readily be calculated. On the contrary, the density of the hollow carbonaceous particles from the cyclone fraction can not be determined readily. Therefore, these particles were analyzed at a rather low electron energy of 15 keV at which the imaging conditions were optimum. From the inner structure of the large spheres, it can be

Downloaded At: 19:16 18 January 2011

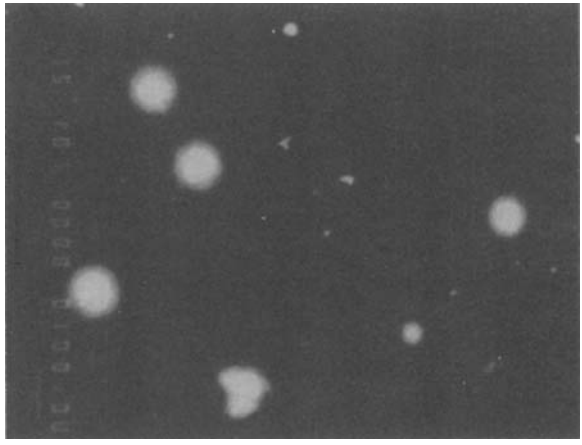

Figure 1 Inverted backscattered electron image (100×) of carbonaceous particles on a silver coated Nuclepore filter.

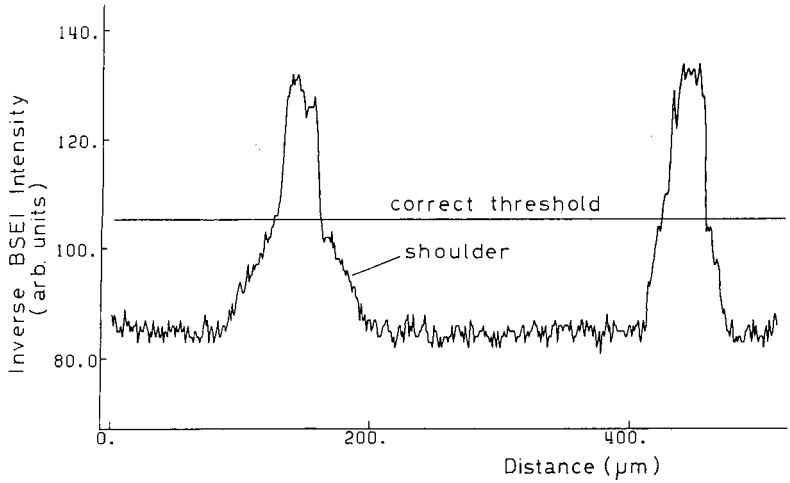

Figure 2 Inverted backscattered electron image profile resulting from a linescan over carbonaceous particles on a silver coated Nuclepore filter.

Downloaded At: 19:16 18 January 2011

estimated that the large voids in the particle are responsible for a total density of the particles far below 1 g/cm^3. When these particles are analysed, only their inorganic composition can be derived from the X-ray spectrum. Consequently, the density estimated in the standardless ZAF correction program should be a severe over-estimation of the true particle density as both the carbonaceous fraction and the voids are not taken into account. Therefore, a first estimate of the elemental composition was calculated by feeding into the standardless ZAF program a density equal to one tenth of the density calculated from the inorganic composition.

A more accurate approximation of the average particle density was obtained by multiplying the initially calculated density (based on the element composition) with a correction factor which was defined as the ratio of the mass of the particles (obtained by weighing) to the mass calculated, using the measured diameter and the initially estimated particle density.

The use of this contrast correction factor α for all particles within one sample, implies that the weight ratio between undetectable elements and the detectable constituents is constant and also that

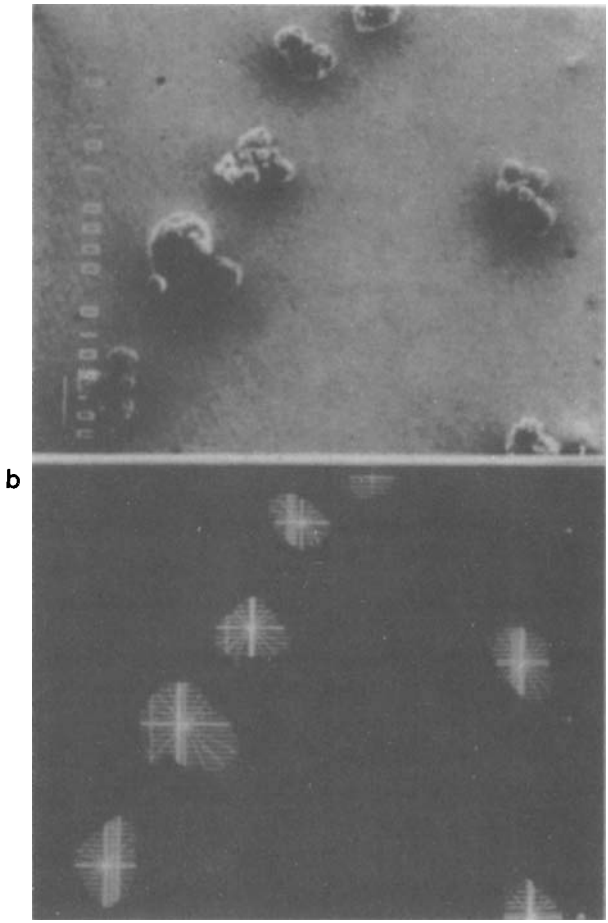

Figure 3 a: Secondary electron image (100×) of a group of carbonaceous particles. b: Electron beam patterns describing the automated localization of the particles shown in a.

the ratio between the total particle volume and the volume of the voids is constant.

EXPERIMENTAL CONDITIONS

The experimental conditions are summarized in Table 1. The maxi-

Downloaded At: 19:16 18 January 2011

Table 1 Experimental conditions during the sample preparation and the particle analysis

	Sample	*Number of particles analysed*	*Number of fields scanned*	*Loading particles/mm²*	*Mass dispersed on the filter (μg)*	*Magnification*
Cyclone fraction	331	800	17	51.4	94	100
	332	800	39	22.4	74	100
	333	800	41	21.3	70	100
	334	800	42	20.8	120	100
	335	647	42	16.8	45	100
	336	484	42	12.6	63	100
	337	217	42	5.6	40	100
	338	268	42	7.0	70	100
	339	321	42	8.4	49	100
	340	322	29	12.1	27	100
	341	800	–	–	–	200
	342	800	–	–	17	200
	343	373	100	16.3	53	200
	344	547	100	24.0	132	200
	345	585	100	25.6	17	200
	346	221	100	9.7	61	200
	347	478	42	11.8	46	100
	348	181	35	5.4	37	100
	349	121	56	2.2	185	100
	350	571	56	10.6	490	100
Filter fraction	331	800	38	2188	16800*	1000
	332	800	8	10368	199296	1000
	333	800	28	2963	21210	1000
	334	800	43	1928	16805	1000
	335	800	37	2241	20285	1000
	336	800	38	2183	13806	1000
	337	800	48	1728	9174	1000
	338	800	11	655	11132	300
	339	800	2	–	8151	300
	340	800	55	1508	9940	1000
	341	800	88	942	10056	1000
	342	800	57	1455	14793	1000
	343	800	81	944	14278	1000
	344	800	45	1843	11249	1000
	345	589	100	610	15600	1000
	346	800	138	601	14340	1000
	347	800	104	797	11682	1000
	348	540	100	560	14350	1000
	349	498	100	516	11733	1000
	350	800	58	1430	13205	1000

*The dispersed sample weight includes the weight of the glass wool from which the particles were removed ultrasonically.

Downloaded At: 19:16 18 January 2011

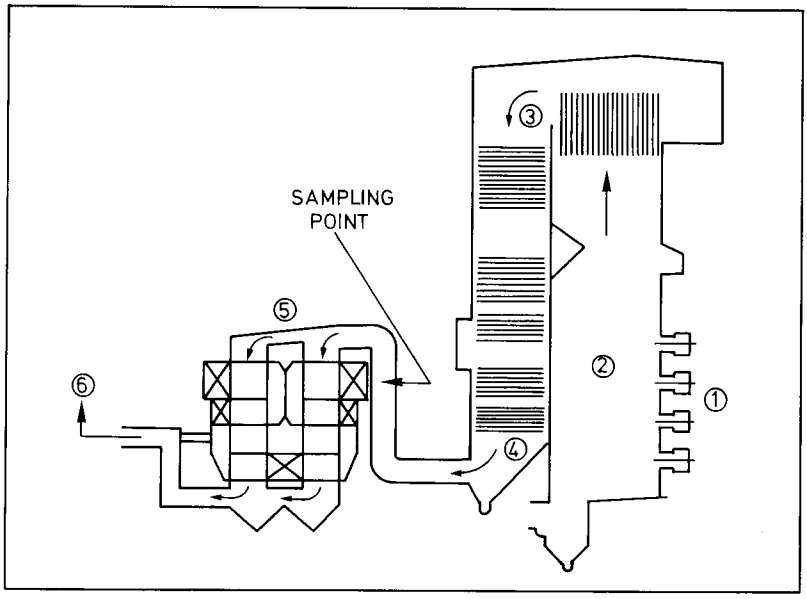

Figure 4 Cross sectional view of the power plant with the position of the sampling point. 1. Fuel injectors; 2. Furnace; 3. Steam generator; 4. Air preheating system; 5. Stack exhaust; 6. Leading to stack.

Downloaded At: 19:16 18 January 2011

mum number of fields analyzed was set at 100 to limit the duration of one analysis to a maximum of 12 hours. In order to prevent agglomeration of the particles, the loading of the cyclone samples was kept rather low and consequently the search of one single particle required up to a few minutes. Also, this low particle density implied a low magnification because otherwise, the analysis would take an unpractically long time. Therefore, the magnification was kept at $100\times$ for the cyclone samples, so that the diameter of the smallest detectable particle was $10\,\mu$m. Analogously, the smallest particle diameter for the filter fraction was limited to $1\,\mu$m.

Sampling

Fly ash samples were obtained by isokinetic sampling with a zero pressure probe (Göthe A.G., Bochum) in a smoke duct before the stack (Figure 4) of the 2×300 MW oil fired thermal power station at

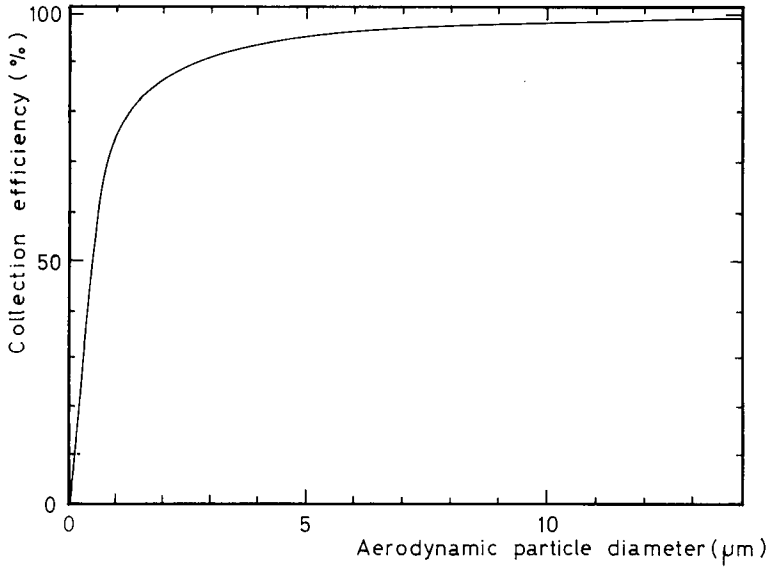

Figure 5 Collection efficiency of the cyclone sampler. (Göthe A.G., Bochum).

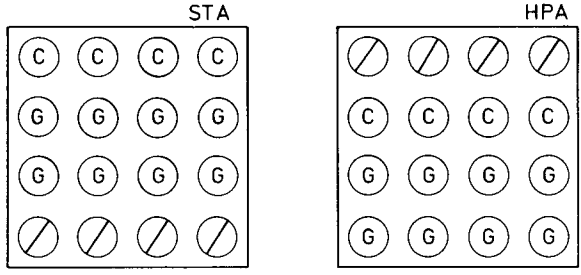

Figure 6 Different burning conditions on the burner array. STA: crude burning under steam atomization; HPA: crude burning under high pressure atomization.

Langerlo (Belgium). The air was sampled isokinetically with an average speed of about 20 m/s and was sucked through a calibrated nozzle to a cyclone and a backup filter. Isokinetic sampling conditions were automatically maintained by the zero pressure probe. The collection efficiency of the cyclone as a function of the aerodynamic diameter is shown in Figure 5.

Figure 6 shows the different burning geometries during the sampling episodes. For the first series of samples the upper row of burners was fed with heavy crude oil using steam atomization (STA).

Downloaded At: 19:16 18 January 2011

The two middle burners were gas fired, and the lower row was not used. During the sampling of the second series, the upper row was not used. On the second row very heavy crude oil was burned under high pressure atomization (HPA) and the two lower rows were gas fired.

After sampling, the cyclone fraction was transferred into airtight bottles because of the hygroscopicity of the material, due mainly to the sulphates present in the fly ash. The glasswool wad from the filter was removed from the sampler and sealed in a PVC tube.

Sample preparation

The quality of the results depends critically on the care taken in this stage of the analysis procedure. Indeed, as the carbonaceous particles have very low densities, and frequently have rather large diameters (20–100 μm), it is often very troublesome to weigh and to handle small amounts in the range of 50–200 μg of powder. This property, combined with the fact that large carbonaceous particles are very fragile objects, make it a difficult task to prepare samples with a size distribution representative for the emissions.

To analyze these samples with an automated image analyzer, particles must be dispersed over a flat and smooth substrate. Irregularities on the substrate surface need to be smaller than 1 μm to avoid the detection of artificial "ghost" particles. Obviously, the best contrast could be created by dispersing the particles on a substrate having a high atomic number, and since the particles must be dispersed by filtration, a silver coated membrane filter proved to be suitable since the X-rays generated by silver did not interfere with the elements detected in the fly ash particles.

Another condition to obtain a representative characterization requires a minimum particle loading on the filter to prevent particle agglomeration. From a particle agglomeration theory,[11] can be calculated that the agglomeration probability is below 0.04 when the particles do not cover more than 1% of the substrate area.

After weighing the bulk fly ash powder in its original glass recipient on a microbalance, the sample is gently shaken manually during 30 seconds in order to disagglomerate the fly ash. A Nuclepore filter (0.4 μm pore size) is coated with a 100 nm thick Ag layer, and mounted on a filtration funnel setup (Millipore S.A.

Downloaded At: 19:16 18 January 2011

Molsheim, France—type XX100 25 00), in a laminar flow hood. In the funnel, 5 ml of a 0.1% rubber cement (Fixogum—Marabu, Marabuwerke, Erwin Martz GmbH & Co, Tamm) solution in *n*-hexane is kept ready. An aliquot of approximately 100 μg fly ash is taken from the bulk, and transferred to the rubber cement solution in the funnel, just below the liquid surface, to stir up the particles. At the same time, the vacuum is applied to start the filtration which takes about 5 minutes. After the end of the filtration, the vacuum is kept during 2 minutes so that the filter can dry up in a clean air stream. Next, the filter is removed from the fritted disk in the funnel, and is mounted on a polyethylene stub with double faced Scotch Tape. Since the filter is coated with a relatively thick silver film even the largest fly ash particles do not show electric charging under the electron beam. Hence, no other conductive coatings need to be applied onto the thus prepared sample.

Downloaded At: 19:16 18 January 2011

To separate the particles of the filter fraction from the glass wool between 10 and 15 mg of the glass wool is immersed in a glass recipient containing 10 ml 0.1% rubber cement solution in *n*-hexane. This immersion is vibrated ultrasonically during 3 minutes and immediately thereafter, an aliquot of 4 ml is taken from this suspension and filtrated on an ASTM sieve of 45 μm to retain single glass fibres that were released by the glass wool in the ultrasonic bath. The sieve is then rinsed once more with 1 ml of rubber cement solution. The sieved suspension can now be brought in a Millipore filtration funnel in which an uncoated Nuclepore filter (0.4 μm poresize) is mounted. After this, the walls of the filtration funnel are washed with blank rubber cement solution and when dry, the Nuclepore filter is mounted on a polyethylene stub, and is coated with 40 nm of carbon. For all samples, the mass of the dispersed particles is listed in Table 1.

RESULTS

Study of individual fly ash particles

Typical examples of particles of the cyclone fraction are shown in Figure 7. The first type has an approximately spherical shape with numerous craters on the surface, suggesting a hollow spongy

structure. The surface itself is smooth but sometimes it is severely deformed because of the influence of the high temperature process it went through. A second particle category, instead of a smooth surface, shows a foamy structure. Some particles have an appearance intermediate between the first and the second type, indicating a possible transition from the first type into the second during the burning process.

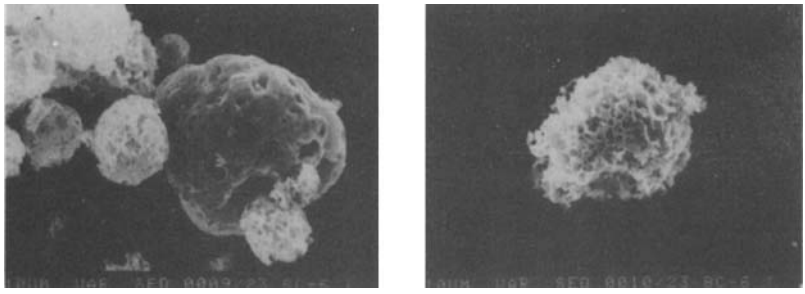

Figure 7 Secondary electron images (400 ×) of particles collected by the cyclone: left: Spongy particle type, right: Foamy particle type.

In the backscattered electron image, these particles have a very low intensity, comparable to that of organic matter. However, very bright spherical particles with diameters below 2 μm can be detected on the surface of the large spongy particles.

Element mapping over a single particle, using wavelength dispersive X-ray emission spectrometry, showed that sulphur and vanadium are dispersed homogeneously in the particle (Figure 8). However, for the latter element a higher concentration was found on specific locations where smaller particles are adhered to the surface. Other elements such as Ti, Fe and Ni were also detected in these small particles. LAMMA analyses previously yielded evidence for the carbonaceous nature of these particles, and also for the presence of oxides of sulphur and vanadium.[4]

From all these observations, it can be stated that the large fly ash particles contain a very porous carbonaceous matrix in which sulphur and several metals are dispersed. It can be expected from the foamy inner structure, that the density of these particles must be very low.

Downloaded At: 19:16 18 January 2011

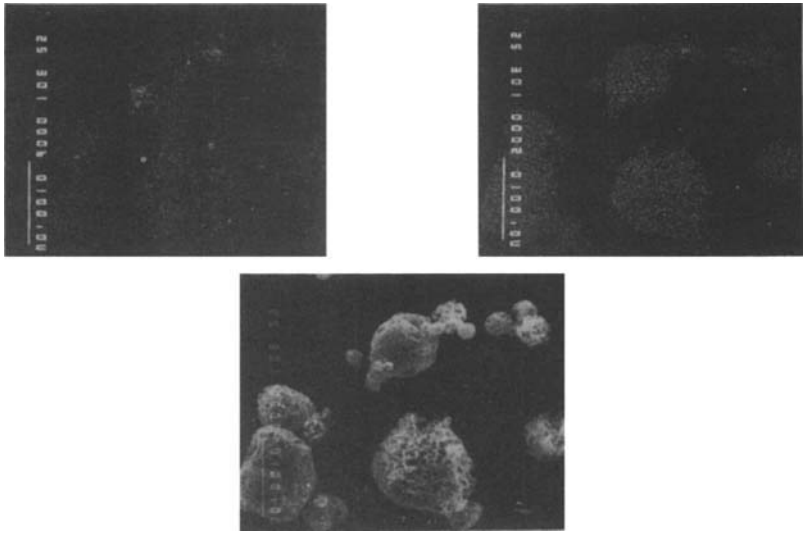

Figure 8 Secondary electron image (left) and wavelength dispersive X-ray emission element mapping of sulphur (middle) and vanadium (right).

The particles from the filter fraction are small (1–5 μm) and mostly have either a spherical or else a polyhedral morphology. Most of the particles of the spherical type contain V, Fe, Ni and some S, but also silicate particles were found. The polyhedral particles typically contain sulphur, presumably as sulphates of the alkali elements. Further, all particles seem to be massive without apparent voids, except for some debris of damaged particles that were probably blown from the cyclone to the filter. Only a rather brief description of these particles was found in literature,[1,2,3] mentioning colour and chemical composition of a few size classes.

Particle size distributions

Typical size distributions of cyclone and filter fraction are shown in Figure 9. As could be expected from the collection efficiency of the cyclone sampler, most of the particles from the filter fraction have an aerodynamic diameter smaller than 5 μm. In the cyclone fraction, particles are found with diameters between a smallest detectable size of ca. 10 μm and 200 μm.

Downloaded At: 19:16 18 January 2011

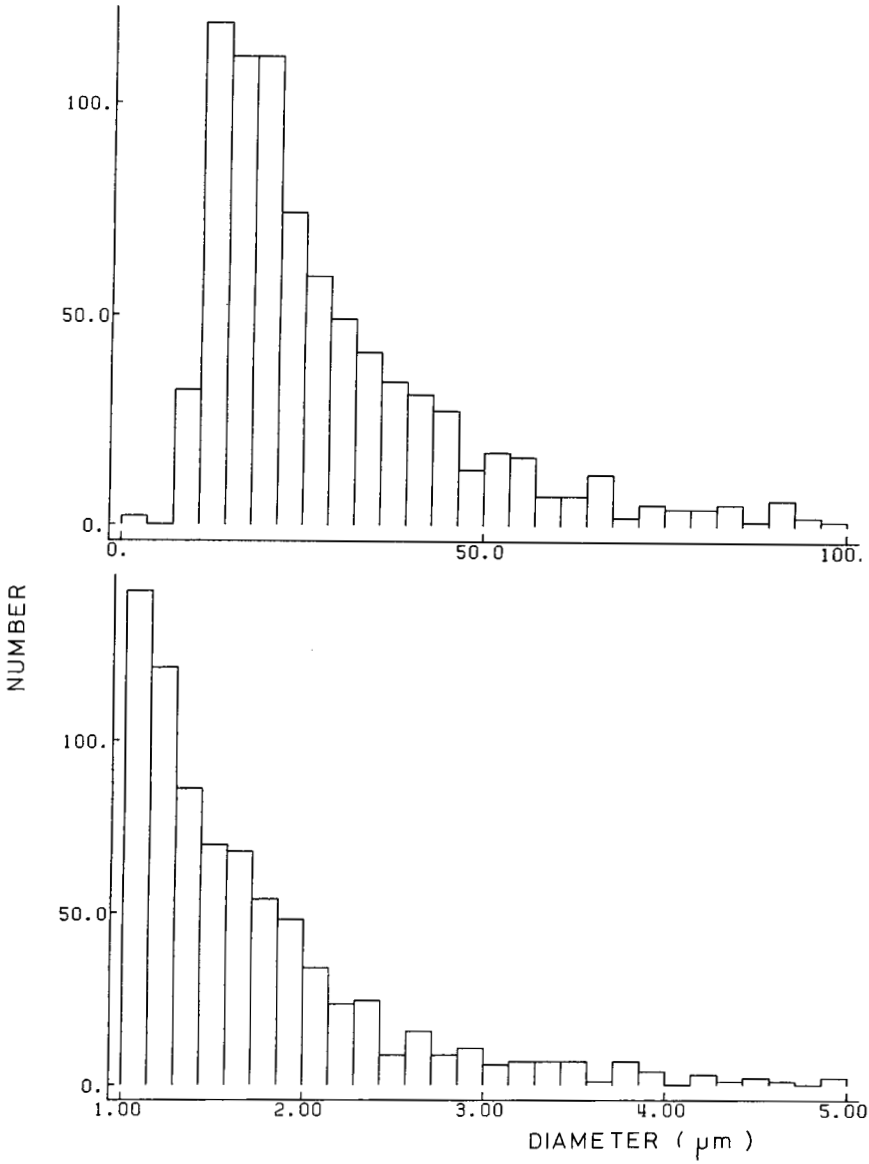

Figure 9 Typical distributions of the cyclone fraction (top) and the filter fraction (bottom).

Downloaded At: 19:16 18 January 2011

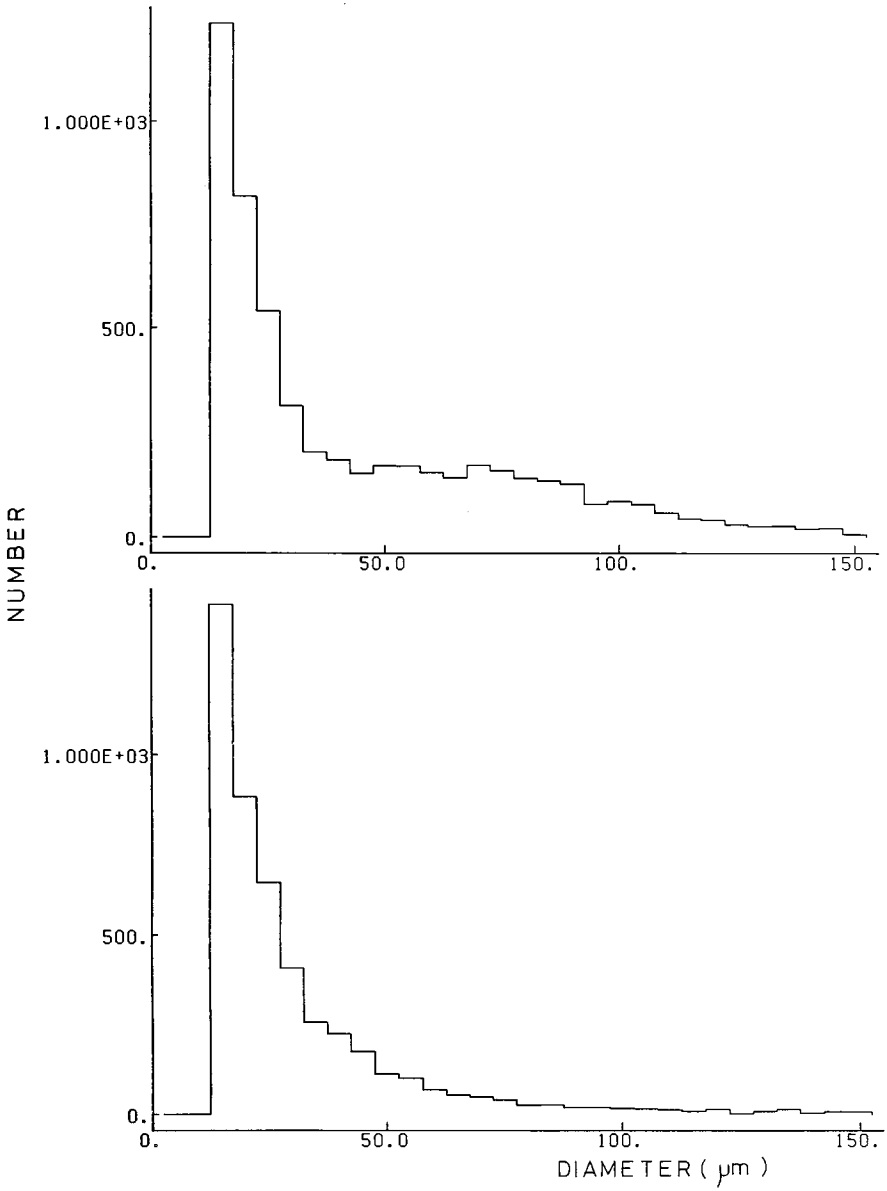

Figure 10 Distribution of the diameter of the particles from all cyclone samples. Top: high pressure atomization; bottom: steam atomization.

Downloaded At: 19:16 18 January 2011

To compare the effect of the burning conditions of the plant on the size distributions, the diameters of all the analyzed particles were classified in four histograms. A first pair of histograms (Figure 10) gives the size distributions of the cyclone fractions that were collected from the plant operated at the two distinct burning conditions and a second pair (Figure 11) shows the distributions of the corresponding filter fractions. Obviously, the particles collected by the cyclone during HPA conditions show a larger abundance of diameters between 50 μm and 100 μm, which obviously means that during the STA crude burning smaller particles are generated. The unexpectedly large number of small ($<30\,\mu$m) particles in the cyclone fraction could originate with fragmentation of larger particles during sampling and sample preparation.

The distribution of the measured diameters of the particles on the filters also shows a significant difference between both burning conditions. For HPA and STA crude burning respectively 3.8 μm and 2.0 μm were found as mean diameters for the filter fraction. This difference is in accord with the results found for the cyclone fraction, and in general it can be concluded that the mean particle size of particles generated by the STA process is significantly smaller than for the HPA process.

Table 2 gives values of the average density of the samples collected during the two test runs of the power plant. Sample 350 also shows an exceptionally high density but this was caused by rather compact particles consisting of conglomerates of smaller carbonaceous particles as followed from electron microscopical inspection. The particles sampled during STA crude burning, show higher densities with a spread over a larger range than those from the HPA burning process. This implies that on the average, particles generated by the steam pulverized crude burning are twice as dense as the particles from crude-gas burning.

Generally, the density of these particles is only about one tenth of the density calculated from their inorganic composition.

A feature which provides information on the efficiency of the burning process is the sulphur to vanadium ratio. Indeed, the higher the vanadium concentration relative to the sulphur concentration, the more the fly ash should approximate the composition of the completely burned ashes, as found in the filter fraction. As an example Figure 12 shows a plot of the sulphur to vanadium ratio as

Downloaded At: 19:16 18 January 2011

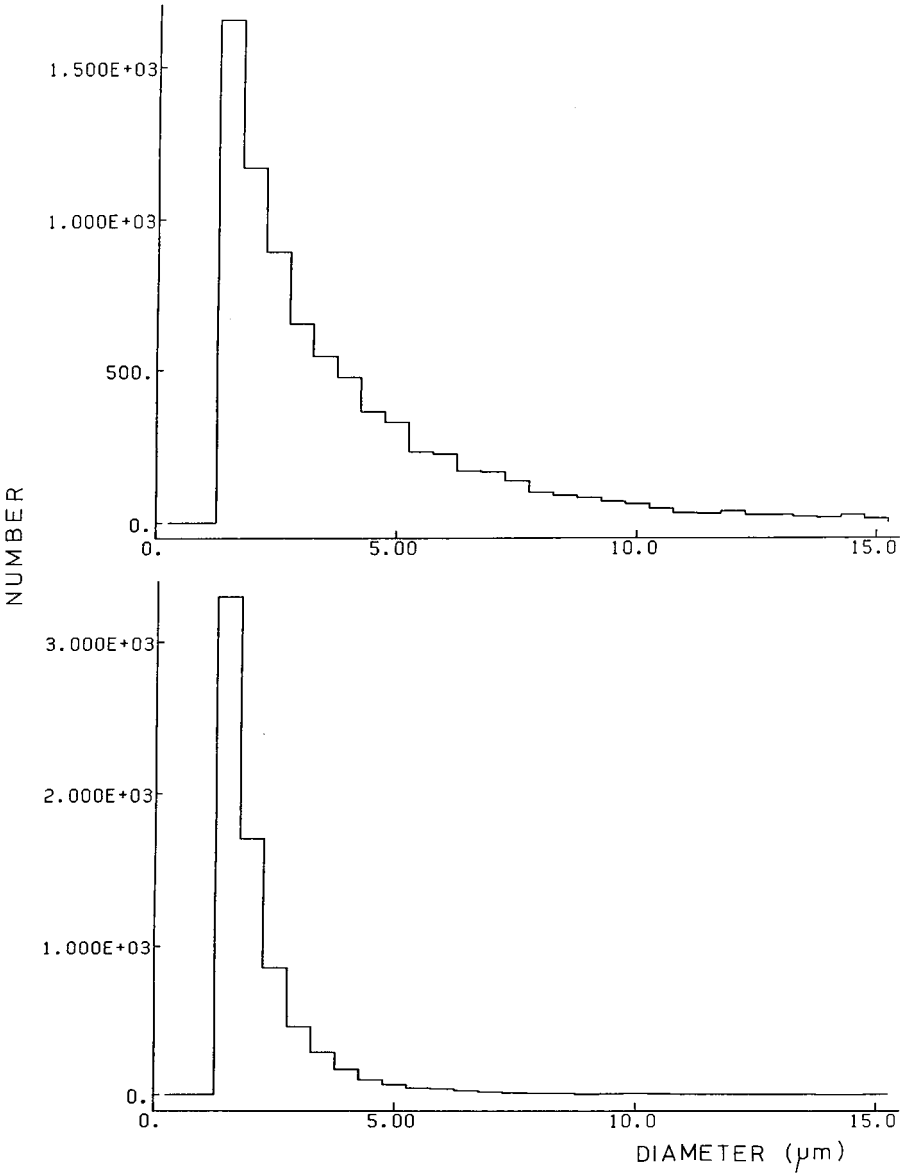

Figure 11 Distribution of the diameters of the particles from all filter samples. Top: high pressure atomization; bottom: steam atomization.

Downloaded At: 19:16 18 January 2011

Table 2 Average density (g/cm^3) of particles in various samples

High Pressure Atomization		*Steam Atomization*	
Sample	*Density*	*Sample*	*Density*
331	0.134	341	–
332	0.054	342	–
333	0.044	343	0.264
334	0.112	344	0.284
335	0.068	345	0.066
336	0.108	346	0.166
337	0.290	347	0.036
338	0.204	348	0.068
339	0.104	349	–
340	0.090	350	0.978
Mean	0.12 ± 0.07	Mean	0.27 ± 0.33

Downloaded At: 19:16 18 January 2011

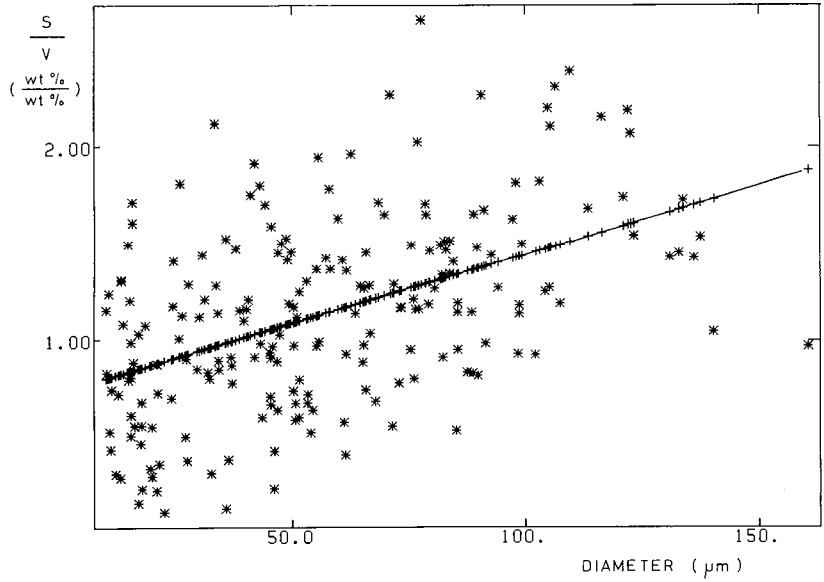

Figure 12 Plot of the ratio S/V of sample 331, with the regression line.

a function of the particle diameter for the cyclone fraction of sample 331 together with its regression line. Regardless the crude burning conditions in all samples a similar increasing trend was observed for the ratio. This supports the hypothesis that both the diameter and the S/V ratio are parameters indicating the extent to which the oil fly ash is burned.

From the density, the calculated particle volume, and finally the elemental concentrations, it is possible to derive the global weight fraction of each element in the total analyzed mass. The results are given in Table 3 for the cyclone fraction, and in Table 4 for the filter fraction. The latter table does not show data for the elements Al, Si, K and Ca, as these elements are also present in the glass wool. Indeed, fragments of fibres (see Figure 6) that were analyzed with the fly ash particles introduced erroneous results for these elements. In Tables 3 and 4 the differences between the results for the different burning processes can clearly be seen. In the cyclone fraction, particles from the STA process can be differentiated from those resulting from the HPA burning process by:

Downloaded At: 19:16 18 January 2011

Table 3 Elemental composition of the cyclone samples (weight %) as calculated from the results of the automated particle analysis. 331–340: High Pressure Atomization, 341–350: Steam Atomization

Sample	*Al*	*Si*	*S*	*Cl*	*Ca*	*V*	*Fe*	*Ni*	*S/V*
331	0.02	1.1	83.0	2.9	0.33	11.6	0.76	0.0	7.15
332	0.09	2.2	76.7	0.66	0.24	19.0	0.57	0.48	4.0
333	0.0	0.23	88.7	0.14	0.16	9.3	0.45	0.92	9.5
334	0.21	0.61	89.8	0.09	0.19	8.8	0.13	0.05	10.2
335	0.10	1.2	77.9	0.27	0.09	18.1	0.71	1.50	4.3
336	0.0	1.26	78.6	0.79	0.31	18.4	0.38	0.20	4.3
337	0.03	0.48	85.5	2.14	0.10	11.7	0.0	0.0	7.3
338	0.0	0.76	83.9	0.10	0.14	14.27	0.10	0.65	5.87
339	0.0	0.59	82.7	0.56	0.11	14.3	1.0	0.68	5.87
340	0.03	0.62	82.2	0.83	0.13	14.7	0.13	0.0	5.6
341	0.31	5.7	51.2	2.0	0.0	22.4	0.1	5.8	2.3
342	0.43	6.1	62.8	0.2	0.5	21.2	4.2	3.4	2.96
343	0.2	15.7	53.6	2.3	1.1	24.2	3.0	0.8	2.2
344	0.5	12.8	51.5	0.04	0.5	16.6	12.1	0.1	3.1
345	0.2	6.8	49.6	0.6	0.3	23.5	15.8	2.3	2.1
346	0.03	7.4	62.2	0.5	1.9	11.5	14.7	0.0	5.4
347	0.1	0.96	81.1	0.7	0.06	13.3	2.9	0.8	6.1
348	0.2	8.6	31.7	9.2	0.2	19.8	25.9	2.3	1.6
349	0.1	1.2	31.6	52.6	0.3	0.0	13.9	0.0	0.0
350	4.1	12.6	21.8	0.9	1.0	4.0	36.5	1.4	5.5

Table 4 Elemental composition of the filter samples (weight %) as calculated from the results of the automated particle analysis. 331–340: High Pressure Atomization, 341–350: Steam Atomization

Sample	*S*	*Cl*	*V*	*Fe*	*Ni*	*S/V*
331	61.2	1.10^{-4}	1.7	0.9	0.4	36.4
332	44.2	0.6	5.4	0.8	0.4	8.2
333	44.3	0.4	7.5	1.2	2.1	5.9
334	36.2	0.0	11.2	1.6	3.8	3.2
335	40.1	0.2	8.2	1.4	2.3	4.9
336	24.5	0.0	6.7	1.5	1.6	3.7
337	35.5	0.0	3.9	0.6	1.1	9.0
338	30.2	5.10^{-4}	10.4	2.1	2.8	2.9
339	13.5	2.10^{-4}	2.1	0.2	0.3	6.4
340	19.2	0.0	3.6	1.0	0.8	5.4
341	5.1	3.10^{-4}	1.8	1.2	0.3	2.9
342	16.7	4.10^{-4}	4.8	5.5	2.7	3.5
343	24.0	0.35	13.5	6.1	7.1	1.8
344	3.8	7.10^{-4}	1.0	0.2	0.4	3.8
345	42.2	3.6	3.9	4.2	6.5	10.9
346	11.0	3.9	1.4	1.5	0.4	8.2
347	14.4	8.2	4.3	17.9	4.2	3.4
348	40.1	8.10^{-4}	8.2	6.4	4.7	4.9
349	12.1	8.7	2.4	5.3	1.7	4.9
350	3.4	0.2	0.3	0.9	0.1	10.5

Downloaded At: 19:16 18 January 2011

—a significantly lower sulphur concentration,

—higher concentrations of Al, Si, Ca, Fe and Ni,

—a significantly higher vanadium concentration.

Evidently, the steam pulverization reduces the sulphur content of these particles.

The filter fraction shows a somewhat different pattern. The sulphur concentration of particles from the STA process is significantly lower, but the vanadium content gives similar figures for both burning processes. The average iron and nickel concentrations for the STA process is somewhat higher than for the HPA process. On the whole, this behaviour is an indication for a better burning of sulphur relative to the metal rich ashes. For the filter fraction the differences between both burning processes are less clear than for the cyclone fraction. This is not entirely unexpected because the smallest particle fraction is the final product of the oil burning processes.

Data on the absolute particulate concentrations in the stack were not available, so that conclusions on the absolute amounts of emitted material could not be drawn.

Magnetic cyclone fraction

Magnetic particles were only searched in the cyclone fraction, since in the filter fraction the particles were mostly attached to the glass wool fibres, and could not be readily removed from them. A simple sampling procedure was applied to separate the magnetic particles from the carbonaceous fraction. A small sample of fly ash was spread out on a clean polyethylene stub and a teflon coated stirring magnet was moved about 3 mm above the sample. After ca. 30 seconds, some particles were observed by the naked eye on the teflon. Using a piece of 3M Scotch Tape the particles were gently captured from the teflon around the magnet. The tape, containing the particles was then mounted on a brass sample holder and coated with carbon.

Observation in the electron microprobe showed that the majority of the particles are large (about 50–100 μm) irregular flakes (Figure 13) with an X-ray spectrum typical for stainless steel. It is extremely unlikely that these particles would have originated from the burning of crude oil. Most probably, these particles therefore originated from the steel walls of the furnace, released by abrasion in this vigorously high temperature process. Since this type of particles was not found

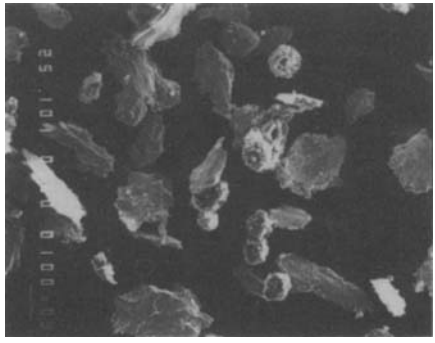

Figure 13 Secondary electron image of the magnetic cyclone fraction (100 ×).

Downloaded At: 19:16 18 January 2011

among about 10000 analyzed particles from the cyclone fraction analyzed without magnetic preseparation, their relative abundance should be very low. On the other hand, the ease with which these particles can be sampled and concentrated on a suitable sample substrate makes this method attractive for the fundamental study and the monitoring of corrosion and abrasion of metal pieces in the interior of such furnaces.

Acknowledgement

This work was carried out with the financial assistance of the National Fund for Scientific Research (NFWO), Belgium.

Downloaded At: 19:16 18 January 2011

References

1. R. J. Cheng, J. R. Hwu, J. T. Kim and S.-M. Leu, *Anal. Chem.* **59**(2), 104A (1987).
2. J. J. Cramer, F. B. Kaylor, J. E. Schmidt and J. R. Zabolotny, *Envir. Sci. Technol.* **11**, 556 (1977).
3. Y. Mamane, J. L. Miller and T. G. Dzubay, *Atmospheric Environment*, **20**, 2125 (1986).
4. E. Denoyer, T. Mauney, D. Natusch and F. Adams, *Microbeam Analysis*, 191 (1982).
5. J. F. Kelly, R. J. Lee and S. Lentz, *Scann. El. Micros. I*, 311 (1980).
6. B. J. Raeymaekers, X. D. Liu, K. H. Janssens, P. J. Van Espen and F. C. Adams, *Anal. Chem.* **59**, 930 (1987).
7. B. Raeymaekers, P. Van Espen and F. Adams, *Mikrochim. Acta II*, 437 (1984).
8. A. Markowicz, B. Raeymaekers, R. Van Grieken, F. Adams, in K. Spurny (Ed.), *Ellis Horwood Ltd.*, (Chichester UK, 1986) pp. 173–197.
9. A. Den Harder and L. De Galan, *Anal. Chem.* **46**, 1464 (1974).
10. B. Raeymaekers, Ph.D. UIA-Antwerp University, Chemistry Department, Universiteitsplein 1, B-2610 Wilrijk, Belgium, 1986, pp. 22–70.
11. S. A. Roach, *Methuen.* London, UK, 1968, pp. 16–21.
12. R. J. Cheng, V. A. Mohnen, T. T. Shen, M. Current and J. B. Hudson, *J. Air Pollut. Control Ass.* **26**, 787 (1976).